Proceedings of the 2008 IEEE
International Conference on Robotics and Biomimetics
Bangkok, Thailand, February 21 - 26, 2009

Design of Pipe Crawling Gaits for a Snake Robot

Thavida Maneewarn and Boonlert Maneechai

Institute of Field Robotics, King Mongkut's University of Technology Thonburi, Thailand

{praew & sam_maneechai}@fibo.kmutt.ac.th

Abstract - **This research aims to study the parameters that contribute to the crawling performance of the snake robot inside an inclined pipe. The shape and motion propagation of the snake robot directly affect the forward crawling speed of the robot inside a pipe. Motion shape code is proposed as the simplified method for describing shape of a modular snake robot. The motion propagation can be created by shifting the code to the adjacent joint. Five different motion shapes were tested on the 12-joints modular snake robot that moved inside a pipe with varied inclined angles. The experimental results showed that the motion shape that has the maximum number of waves along the robot length and the largest basis angle resulted in the fastest forward crawling speed.**

***Index Terms* - Snake robot, Locomotion, Gait design, Pipe Inspection**

I. INTRODUCTION

Snake robot is a hyper degree of freedom robot which has the advantage of its ability to move in various types of terrain and spaces that are difficult to reach. Pipe inspection is one of the industrial applications that the snake robot can be used. A snake robot usually has small diameter, thus can move inside a restricted space such as water pipe, electrical conduit and air duct. Furthermore, a snake robot can also adapt its shape so that it can move in pipes with varying width.

Most of researches focused on motion of a snake robot by analyzing a serpentine motion [1] [2]. However, researches in a specific area of a snake robot motion inside pipes or narrow spaces, can be divided into 3 groups; a hyper-redundant arm, a wheel-supported robot and a modular snake. A hyper-redundant arm used inverse kinematics with an optimization algorithm to solve for the motion solution of the robot [3]. In a wheel-supported robot, all wheels of the robot have to touch the inner wall of the pipe in order to propel the robot forward. In a modular snake, the robot uses a creeping motion [4] [5] or a snake-like form such as a 'sinusoidal wave drive' [6] [7] to create the propelling force for the robot. In the same realm, Chen at al.[8] also proposed the travelling wave locomotion that moved the contacts of the robot joint with the supporting plane along the robot body to obtain the propelling force on flat plane. This paper focuses on finding an appropriate gait for a snake robot to move inside an inclined pipe (up to 90 degrees).We propose the concept of motion shape code which is a discrete and simplified representation of the robot shape and its motion. The robot motion is created from shifting the code along the consecutive robot joint module at the specified interval (the shifting time). Five examples of motion shape code were designed and tested on the snake robot. Experiments were performed to compare the performance of different motion shape codes when the basis angle, the shifting time and the angle of the inclined pipe were varied. The performance of the pipe crawling gait was measured from the maximum inclined angle of the pipe that the robot can move forward and the moving speed.

II. SNAKE ROBOT DESIGN

The snake robot was designed and developed for this study. We are interested in the modular design, where all joints and links of the robot are similar. The modular design allows the robot to easily change its configuration such as the number of joints. The kinematics analysis and the design of the robot is presented in this section.

A. Snake robot kinematics

The snake robot was designed to be the serial linkage mechanism, in which two links were connected by a 1 dof. rotational joint. The kinematic relationship between the robot joint angles and the cartesian position (x-y) can be described in equation (1) and (2). The frame assignment is also shown in fig.1.

$$x = L_1 \cos\theta_1 + L_2 \cos(\theta_1+\theta_2) + ... + L_n \cos(\theta_1 + ... + \theta_n) \quad (1)$$

$$y = L_1 \sin\theta_1 + L_2 \sin(\theta_1+\theta_2) + ... + L_n \sin(\theta_1 + ... + \theta_n) \quad (2)$$

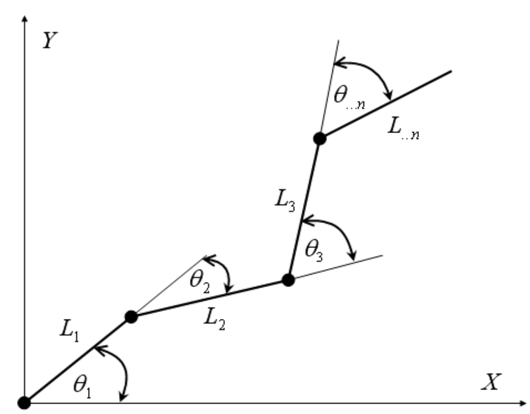

Fig. 1 A snake robot kinematics

B. Snake robot system

The snake robot developed for this study consists of 12 links. Two consecutive links are connected by a revolute joint which is a commercial servo motor (Robotis AX-11). The dimensions of each link are 7 cm long, 4.8 cm high and 3 cm wide. An example of a 4 joints serial snake robot is shown in fig.2. All joints and links are homogeneous based on the modular design concept.

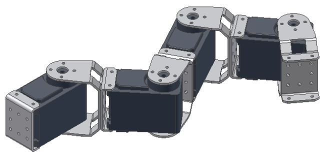

Fig. 2 CAD model of a modular snake robot

The robot system comprises of a computer, a microcontroller board, an external power supply and the snake robot as shown in fig. 3. The high level control such as parameters setting and motion shape selection is performed on the main computer. The control parameters such as motor speeds and angles are sent to the microcontroller board (ATMEL ATMEGA128) via RS232. These data are then sent to all motor in the protocol defined by the motor's manufacturer via a serial bus connection. The position control is performed at the servo motor. The prototype snake robot that was made from aluminium is shown in fig.4.

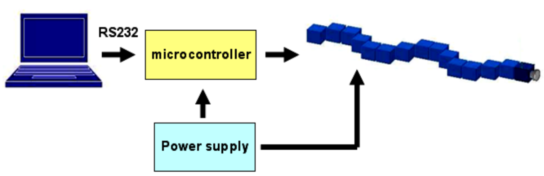

Fig. 3 A system diagram of the snake robot

Fig. 4 The prototype snake robot

III. Mechanism of Pipe Crawling Motion

A. *Physics of pipe crawling*

Pipe crawling has a distinctive characteristic due to the fact the pipe wall naturally creates a position constraints for the robot. In the specific study of a motion for a snake robot inside the pipe, the robot uses the frictional force created between the robot and the inner surface of the pipe to propel the robot forward. In the analysis of serpenoid motion of a snake robot on flat plane [1], the propelling force is generated from the directional surface of friction created by the robot which is usually obtained by attaching the passive wheels underneath the robot's body. For the in-pipe crawling motion, instead of using the directional surface of friction, the force that propel the robot forward came from the static friction force that prevents some contact points between the robot's body and the inner wall of the pipe from slipping. The shape of robot at each instantaneous of time determines the point of non-slipping contacts and the amount of changes of robot's body position over time. In the case of an inclined pipe, the gravitational force affects the forward motion of the robot which directly relates to the inclined angle of the pipe as shown in figure 5.

The shape of robot that changes over time creates the changing position of non-slipped contact points. The shape of robot also determines the direction of force that the robot applies to the wall. If the direction of this force is within the friction cone (i.e. depends on the coefficient of friction of the contact point/surface between the robot and the wall), the non-slipped contact can be successfully established. The friction cone is defined as shown in eq.(3)

$$\gamma = \tan^{-1} \mu \tag{3}$$

when μ is the coefficient of friction

γ is the friction angle of a friction cone

Figure 6. shows two different motion shapes, where the left hand image shows the shape that has the smaller angle between the robot body and the wall than the one in the right hand image. If the force that the robot acts on the wall is outside of the friction cone, it could make the contact point slip. If the robot is slipping at the contact point, then the robot cannot propel forward inside the pipe.

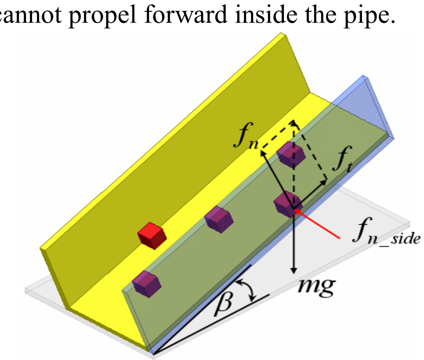

Fig. 5 The force diagram at the non-slipped contact point

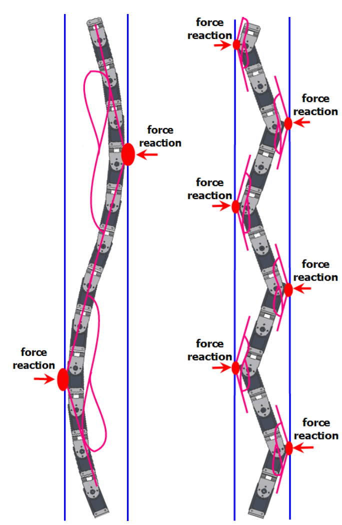

Fig. 6 The relationship between forces generated by motion shape and friction cone of the surface that resulted in the non-slipped contact points

B. Motion shape code

Motion shape code is the discretized and simplified way to described the shape and motion propagation of a serial modular snake. The angular position of each joint corresponds to an integer that represents the multiplication factor to the basis angle and can be calculated in (4).

$$\theta_i = C_i * \alpha \tag{4}$$

θ_i : angular position of joint *i*

C_i : integer number *ith* in motion shape vector

α : basis angle

The motion shape vector is the vector of length *n,* where *n* is the number of joints in the modular snake robot. Each element of the motion shape vector is an integer code that is assigned to each joint which is sent to the motor at every shift time interval. After one cycle (*nth* data are sent) is complete, the data in the motion shape vector is performed the left or right cyclic-shifted to the adjacent slot to create the forward or backward propagation of motion along the snake robot's body. Example can be shown in figure 7, the motion shape is specified as [1,-1,1,-1,1,-1,1,-1,1,-1,1,-1] The basis angle is 60 degrees, the angular positions for joint 1 to 12 will be [60,-60,60,-60,60,-60,60,-60,60,-60,60,-60] degrees. If the shift time is set to 100 msec, the angular position will be sent to each joint at every 100 msec, until all 12 joints angle are updated. The motion shape vector is then assigned to the new value by left-cyclic shifting to [-1,1,-1,1,-1,1,-1,1,-1,1,-1,1] and the angular positions for joint 1 to 12 will be assigned to the new values of [-60,60,-60,60,-60,60,-60,60,-60,60,-60,60] degrees and then again the joint angle will be sent to the robot at every 100 msec time interval. The motion shape code represents the basic shape of the snake robot module where the basis angle and the shift time are variables that can be adjusted according to environment.

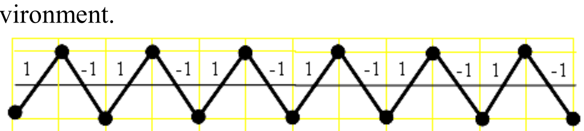

[1,-1,1,-1,1,-1,1,-1,1,-1,1,-1]

Fig. 7 The example of motion shape code

In designing the pipe crawling gait for the snake robot, it is necessary to create the shape that can guarantee at least two contact points between the robot's body and the inner wall of the pipe at all times. These non-slipped contact points are necessary for creating the forward motion. The basis angle for each shape is selected based on the geometrical diagram shown in fig.8 and eq.(5). The basis angle is calculated from the width of the pipe to ensure that the minimum numbers of contact points are maintained during the robot motion.

$$D = L\sin\left(\frac{\alpha}{2}\right) \tag{5}$$

When, D is the width of inner pipe walls, L is the length of straight segments of the robot and α is the basis angle.

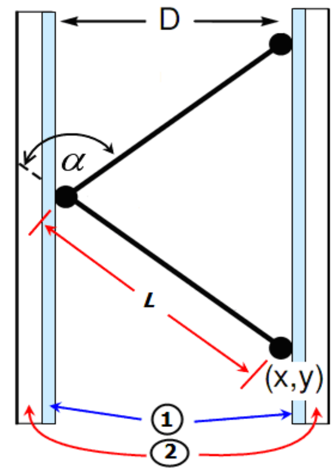

Fig. 8 The geometrical relationship of the basis angle and pipe with (1) indicates the compliant inner wall of the pipe, (2) indicates the rigid outer wall of the pipe.

IV. EXPERIMENT

The experiment was designed to test the performance of different motion shape codes for pipe crawling. The relationship between different parameters of the crawling gait and the speed was the main focus of this study. The parameters of the crawling gait that were studied in this experiment were the number of contact points, the basis angle (α) and the effective length along the axis of the pipe for each shape, thus 5 motion shapes were studied. These 5 motion shapes have different number of waveforms per 12-joint length as shown in figure 9.

TABLE I

FIVE MOTION SHAPE VECTORS USED IN THIS EXPERIMENT

Motion shape	Motion shape vector
case I	[-1,-1,-1,-1,-1,-1,1,1,1,1,1,1]
case II	[-1,-1,0,1,1,0,-1,-1,0,1,1,0]
case III.I	[-1,-1,1,1,-1,-1,1,1,-1,-1,1,1]
case III.I	[-1,0,1,0,-1,0,1,0,-1,0,1,0]
case IV	[-1,1,-1,1,-1,1,-1,1,-1,1,-1]

The motion shape vector corresponding to each motion shape is shown in table I. The number of waveforms directly relates to the number of contact points and the basis angle of each motion shape. For a given pipe inner width (D=6.2cm), the basis angle α for each motion shape was calculated from equation (5) as shown in table II.

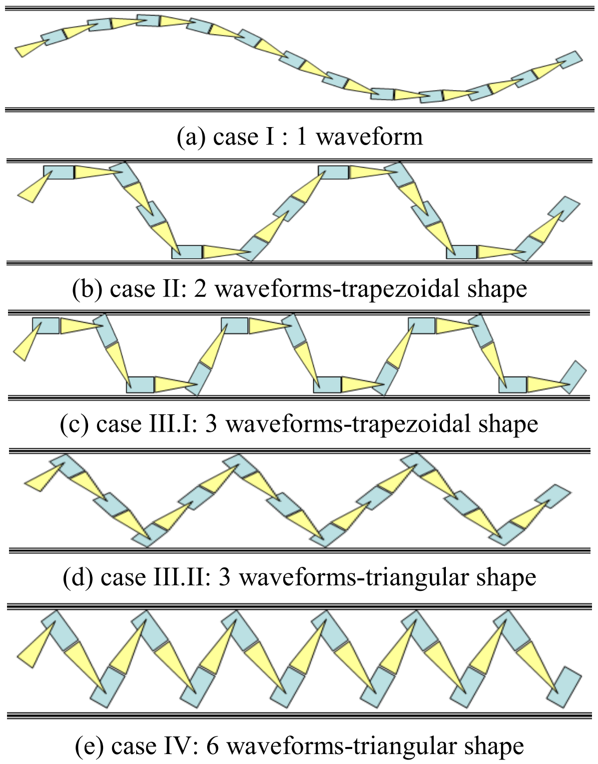

Fig. 9 Five cases of motion shape in the experiment a) case I b) case II c) case III.I d) case III.II e) case IV

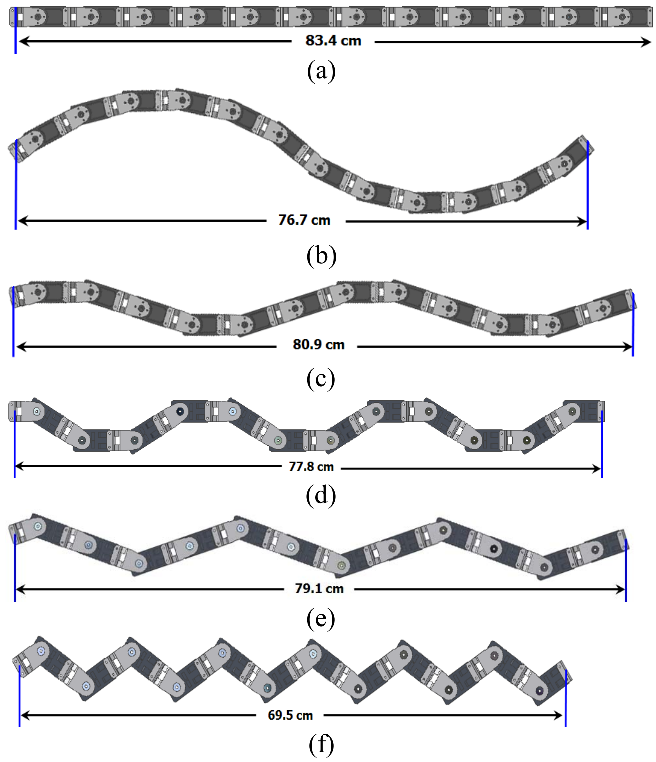

Fig. 10 The geometrical effective length of the robot along the pipe axis (a) full length (b) case I (c) case II (d) case III.I (e) case III.II (f) case IV

Figure 10 shows the effective length measurement from the geometrical relationship for a given motion shape and basis angle. Note that in case I, the effective robot length inside the pipe became larger than this measurement because the pipe wall constrained the robot from reaching the specified command angle. The forces that the robot acted toward the wall allow the robot to maintain the non-slipped contact. However, the actual effective length inside the wall in this case is 81.8 cm which was larger than the geometric length.

TABLE II
PARAMETERS SETTING FOR DIFFERENT MOTION SHAPE

Motion shape	Basis angle α (deg.)	Shift time (msec.)	Number of contact points	Effective length along pipe axis (cm)
case I	13	10	2	76.7 *
case II	17	10	4	80.9
case III.I	30	20	6	77.8
case III.II	37	20	6	79.1
case IV	67	70	12	69.5

* the actual length measured when the robot was in the pipe was 81.8 cm

In this experiment, the pipe was constructed from two rigid plates with rubber foam attached to the inner side of the wall as shown in figure 11.The pipe is 150 cm long. The width of inner pipe wall (D) = 6.2 cm. The thickness of the inner wall material = 1.4 cm. The rubber foam, which is a compliant material with large friction coefficient, was chosen so that the non-slipped contact can be easily established. The estimated coefficient of friction of the inner wall surface is 0.781, therefore the friction angle of friction cone that is calculated from (3) is 37.9°. From the selected motion shape in five cases, the force generated at the contact point in all motion shapes satisfied the friction constraint, thus the non-slipped contact can be established. The pipe inclined angle was assigned in 10 degrees incremental step from 0 to 90 degrees for each test.

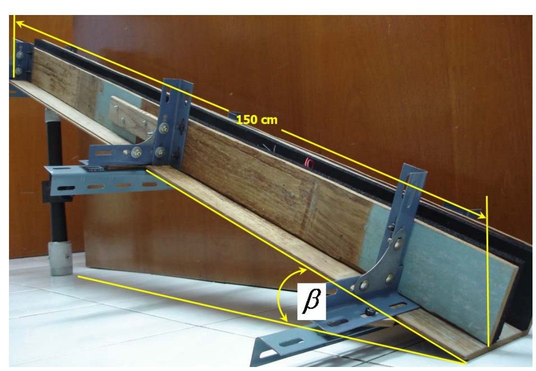

Fig. 11 The inclined pipe used in the experiment

Fig. 12 The prototype robot in the experiment

In the experiment, the 12-joints modular snake robot was assigned the motion shape according to different parameters setting shown in table II. Fig. 12 shows the image of the robot in the pipe during the experiment. The crawling velocity of the robot was measured and the result is shown in fig. 13.

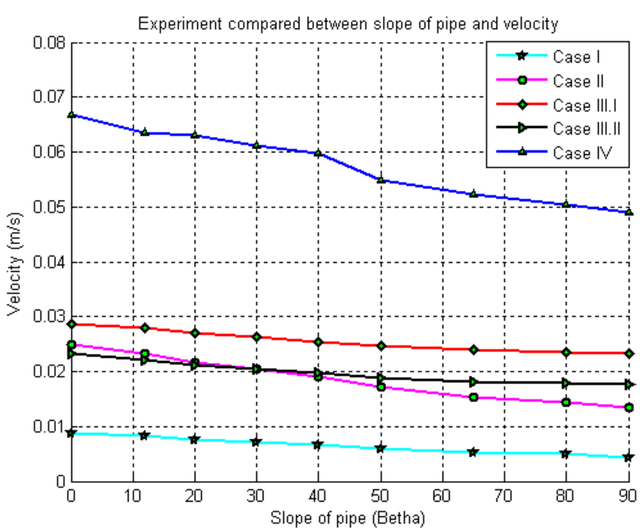

Fig. 13 The graph between crawling velocity (m/s) and inclined angle of the pipe (degrees) for each motion shape: case I, II, III.I, III.II and IV

Results of the experiment showed that case IV has the fastest crawling speed compared to other motion shapes in all inclined angles. Under the non-slipped contact condition, the crawling speed directly depends on the effective length of the robot. Experimental results also showed that the forward crawling velocity decreased with the larger inclined angle of the pipe. The reduction of crawling velocity due to the larger inclined pipe angle was more apparent in case IV when compared to other cases. In case III.I and III.II, where the numbers of contact points were the same, but the shape, the basis angle and the effective length were different, case III.I has the higher crawling velocity than III.II. Since the effective length of case III.II is larger than III.I, therefore the factor that mainly contributed this difference in speed was the effective length of the shape.

V. Conclusions

In this paper, the crawling motion of a modular snake robot in an inclined pipe was studied. The crawling motion in the pipe can be generated by creating a non-slipped contact point between the robot and the inner pipe wall. The non-slipped contact depends upon the static friction coefficient between the robot and the inner wall of the pipe and the direction of force that the robot applies to the wall. When the sufficient amount of force is applied by the robot to the wall and the direction of force lies within the friction cone, the non-slipped contact condition can be established. The motion shape code is proposed as the discretized and simplified method for describing shape and motion of the robot. The crawling motion is generated by shifting the motion shape vector at the end of each update cycle. The experiment was performed to study the relationship between different parameters of the motion shape and the crawling velocity of the robot in an inclined pipe. From 5 different selected motion shapes, the motion shape that has the largest number of waveforms along the length of the robot has the fastest crawling speed. This motion shape has the shortest effective length along the axis of the pipe, which contributes to its gaining distance per one cycle. With the crawling gaits suggested in this paper, the non-slipped contact point is the necessary condition for the robot to propel itself inside the pipe. As long as this condition is maintained, the effective length of its motion shape is the main factor for achieving the high crawling speed.

Acknowledgments

The authors would like to thank Dr.Djitt Laowattana for his valuable suggestions. This research project was supported by the Office of the National Research Council of Thailand.

References

[1] S. Hirose, “Biological Inspired Robots snake-like locomotors and manipulators”, OXFORD pp.75-84, 1993.

[2] M. Mori and S. Hirose, “Development of Active Cord Mechanisms ACM-R3 with Agile 3D mobility” Proceeding of the 2001 IEEE/RSJ International Conference on Intelligent Robot and Systems Maui, Hawali, USA, Oct.29 – Nov.03,2001.

[3] M.W. Hannan, and I. Walker, “The ‘Elephant Trunk’ Manipulator, Design and Implementation” Proc. of the 2001 IEEEUASME International Conference on Advanced Intelligent Mechatronics, Italy, 2001.

[4] A. Wolf, H. B. Brown, R. Casciola, A. Costa, M. Schwerin, E. Shamas, H. Choset, “A Mobile Hyper Redundant Mechanism for Search and Rescue Tasks” Proceedings of the 2003 IEEE/RSJ Intl. Conference on Intelligent Robots and Systems Las Vegas, Nevada · October 2003.
[5] A. Shapiro, A. Greenfield, H. Choset, “Frictional Compliance Model Development and Experiments for Snake Robot Climbing” Proceeding of the 2007 IEEE International Conference on Robotics and Automation Roma, Italy, 10-14 April 2007.
[6] A. Kuwada, Y. Adomi, K. Suzumori, T. Kanda, S. Wakimoto, N. Kadowaki, “Snake-like Robot Negotiating Three-Dimensional Pipelines” Proceeding of the 2007 IEEE International Conference on Robotics and Biomimetics, Sanyn, China, 15-18 December 2007.
[7] S. Wakimoto, J. Nakajima, M. Takata, T. Kanda, K. Suzumori, “A Micro Snake-like Robot for Small Pipe Inspection” Proc. of the IEEE International symposium on Micromechatronica and human science, pp. 303-308,19-22 October 2003.
[8] L. Chen, Y. Wang, S. Ma, B. Li, “Analysis of Traveling Wave Locomotion of Snake Robot” Proceeding of the 2003 IEEE International Conference on Robotics, Intelligent Systems and Signal Processing, Changsha, China – October 2003.